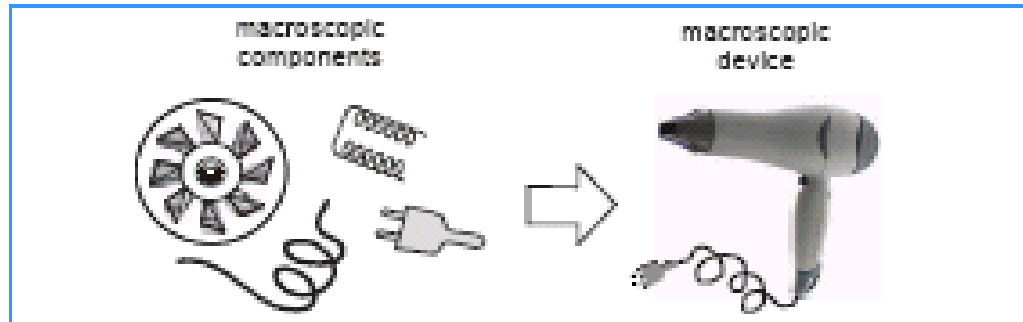
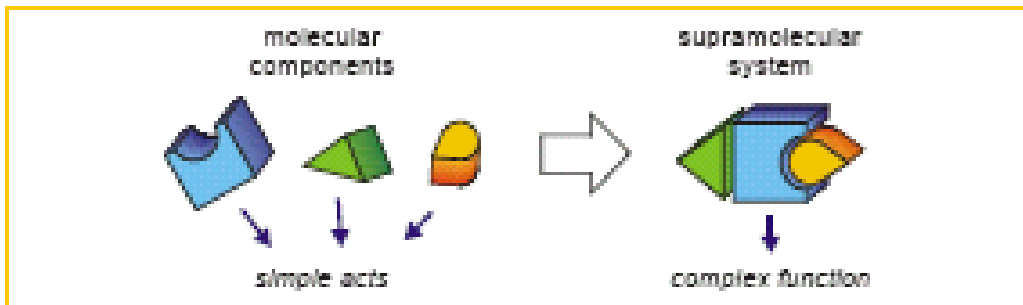


Dispositivi e Macchine Molecolari

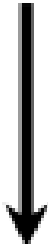
Macroscopic device



Molecular-level device



**design +
synthesis**



**Molecular
Components**



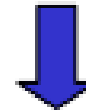
**self-assembly,
self-organization**

or

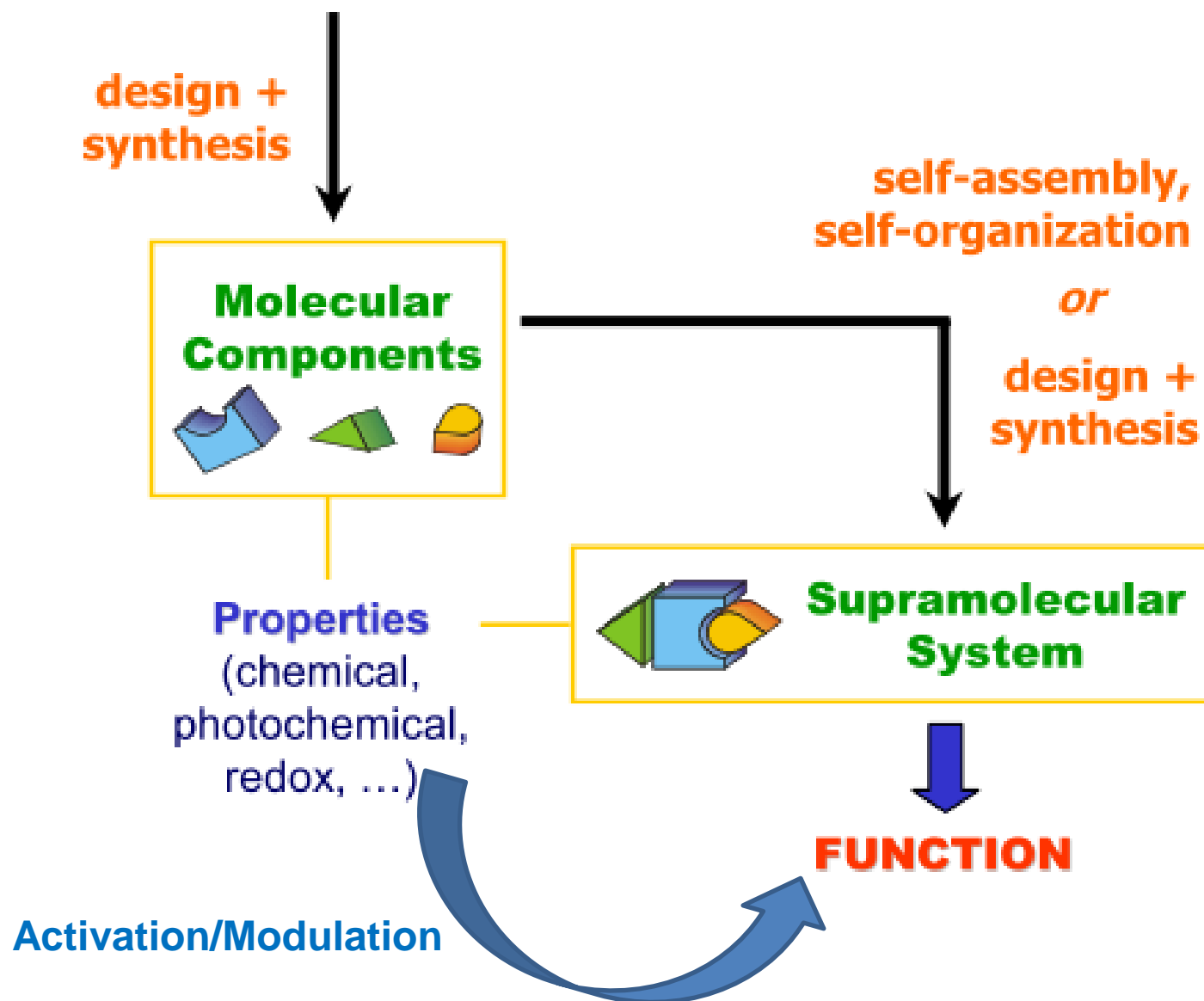
**design +
synthesis**



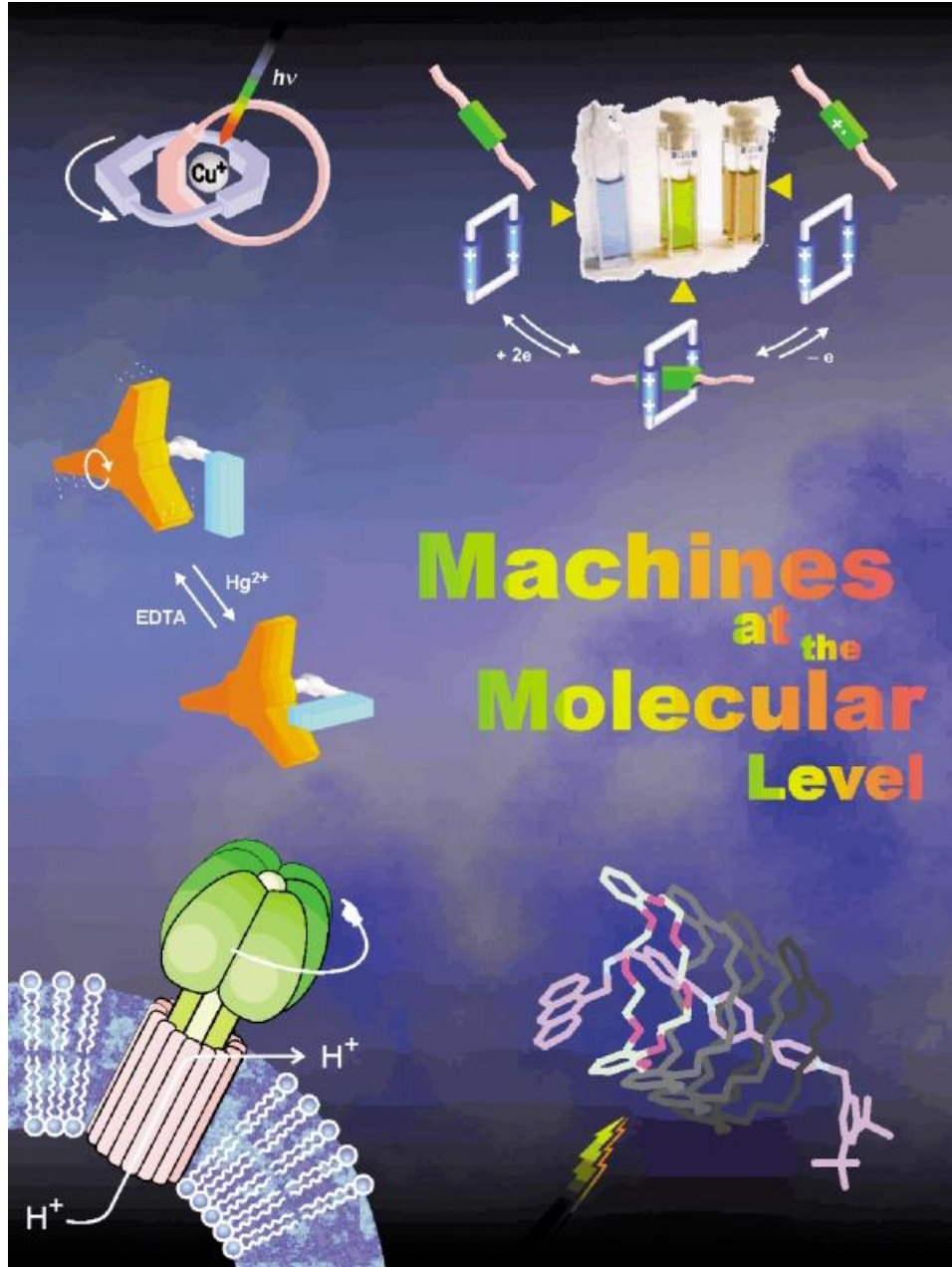
**Supramolecular
System**



FUNCTION



- tipo di energia (chimica, fotoni, elettroni)
- monitoraggio (tecniche fotofisiche, elettrochimiche)
- processo ciclico
- tempo (picosecondi-minuti)
- funzione



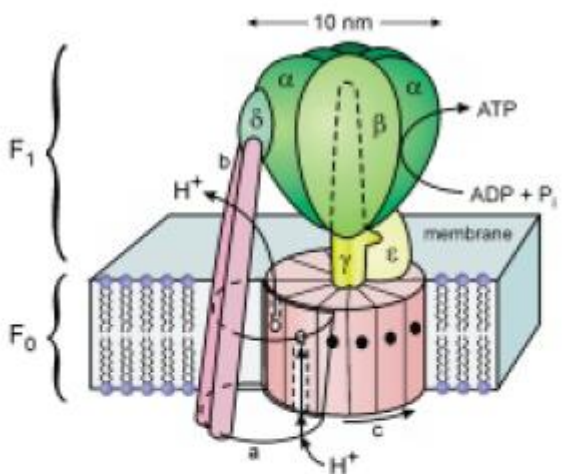


Figure 1. The structure of F₀F₁ATP synthase.^[18] The catalytic region is composed of the subunits α - ϵ . The proton channels lie at the interface between the subunits α and c (dashed lines indicate the putative inlet and outlet channels). Proton flow through the channels develops torque between the α and c subunits. This torque is transmitted to F₁ via the γ shaft and the ϵ subunit, where it is used to release ATP sequentially from the catalytic sites in F₁. The c subunit consists of 9–12 twin α -helices arranged in a central membrane-spanning array. The α subunit consists of 5–7 membrane-spanning α -helices and is connected to F₁ by the b and δ subunits. Reprinted by permission from ref. [16] (Copyright[®] Macmillan Magazines Ltd 1998).

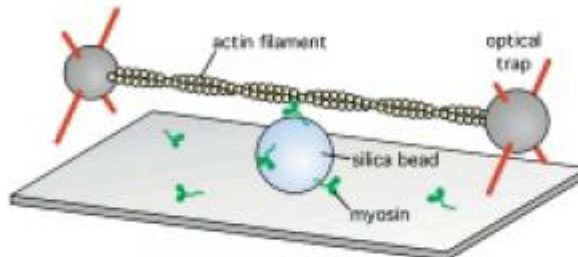
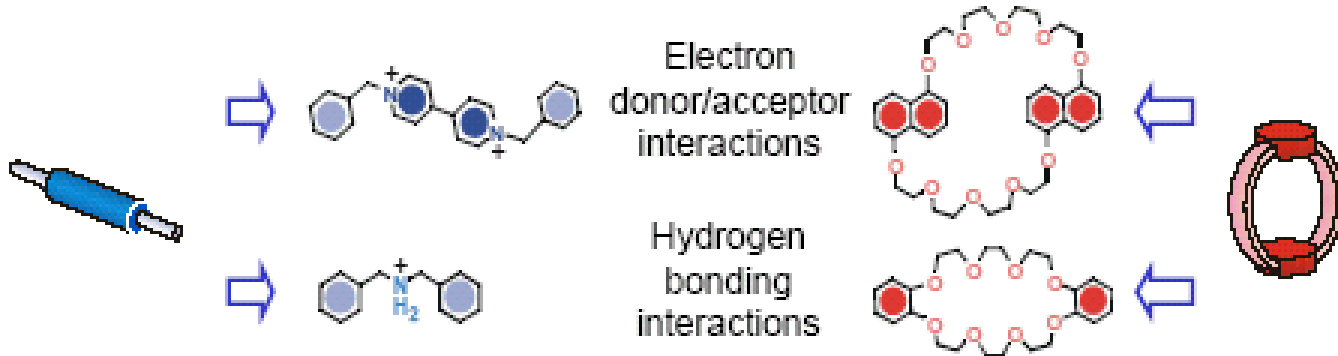
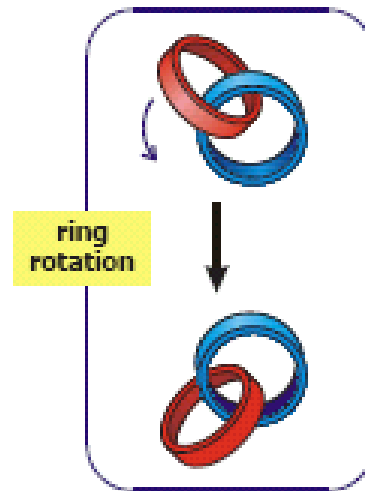
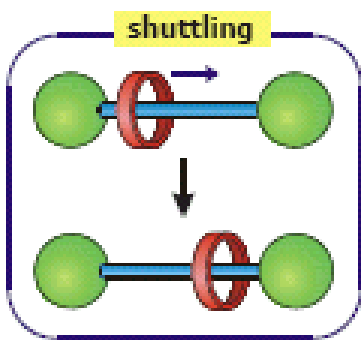
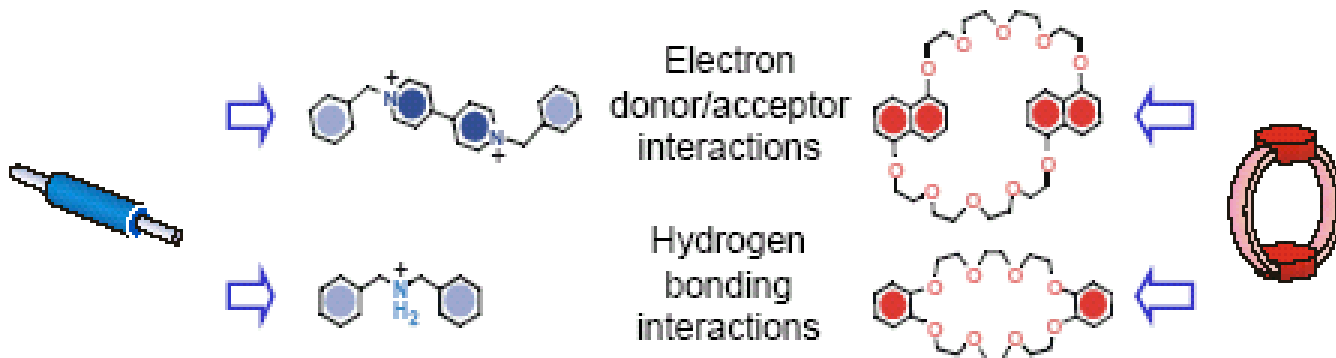
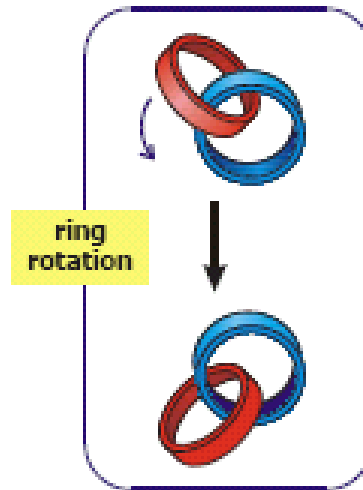
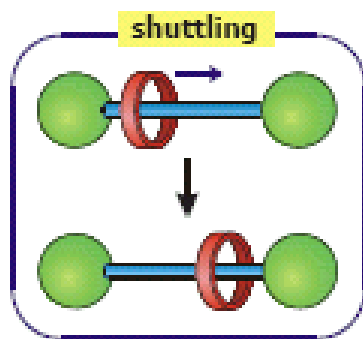
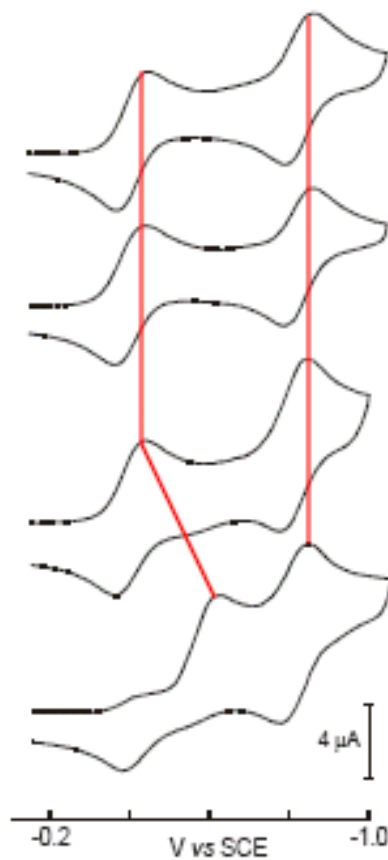
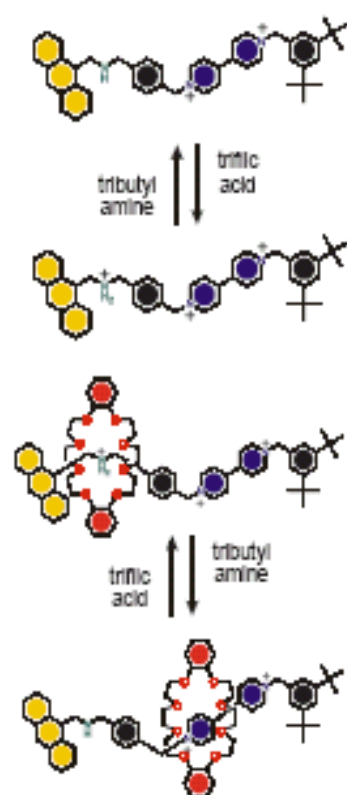
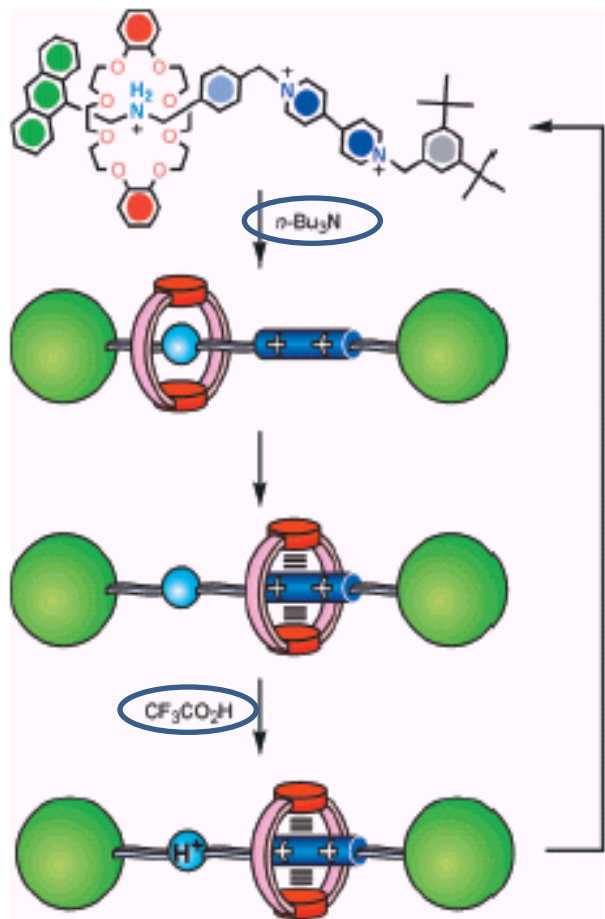


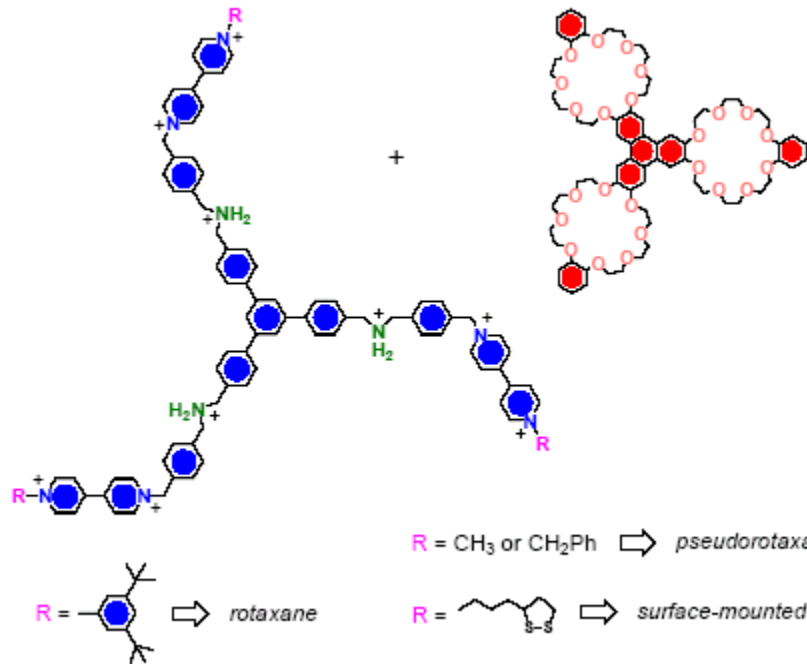
Figure 2. Experimental geometry used^[19] to observe single myosin molecules binding and pulling an actin filament. The filament was attached at either end to a trapped bead. These beads were used to stretch the filament taut and move it near surface-bound silica beads that were decorated sparsely with myosin molecules. Adapted with permission from ref. [19] (Copyright[®] Macmillan Magazines Ltd 1994).





Input chimico





Ascensore molecolare

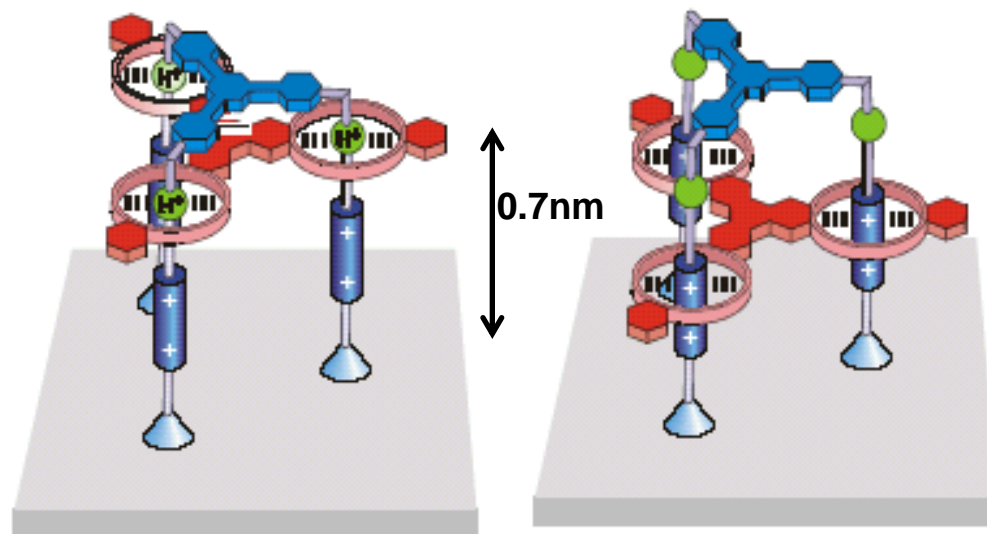
Strong $\text{N}^+ \cdots \text{O}$

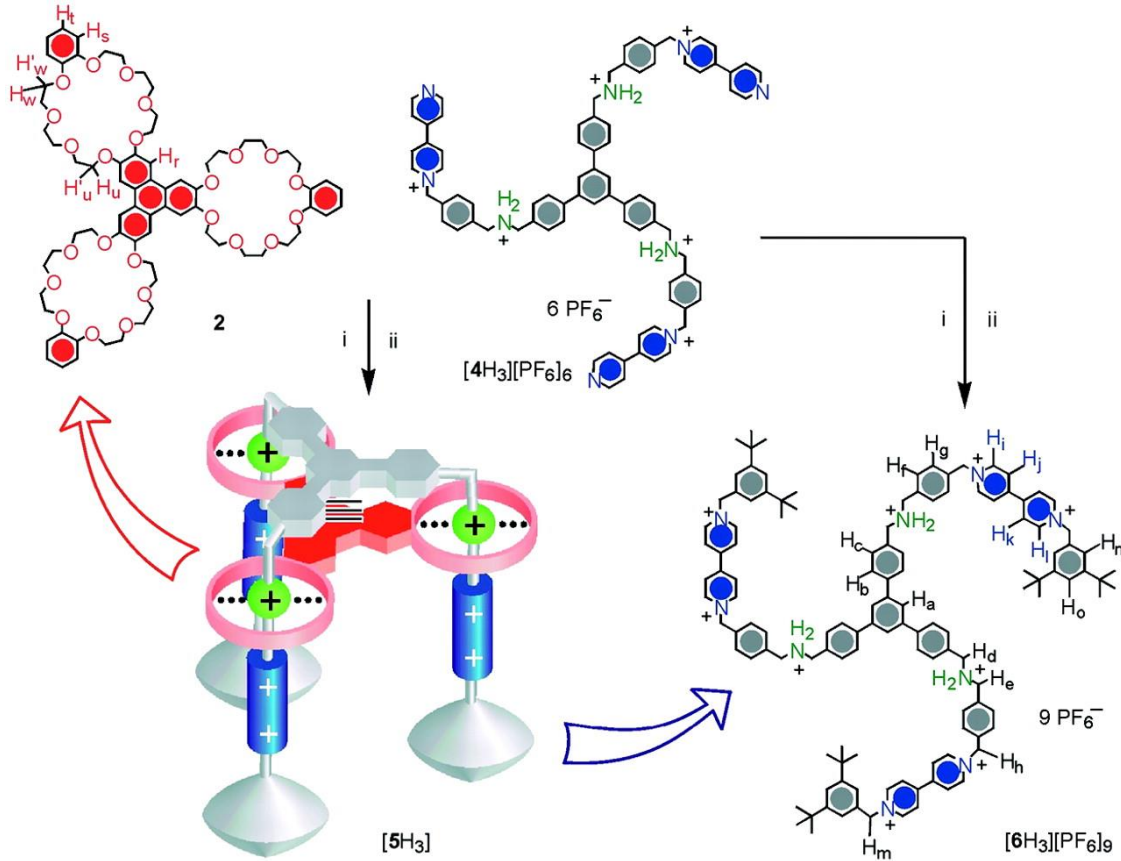
$\pi - \pi$

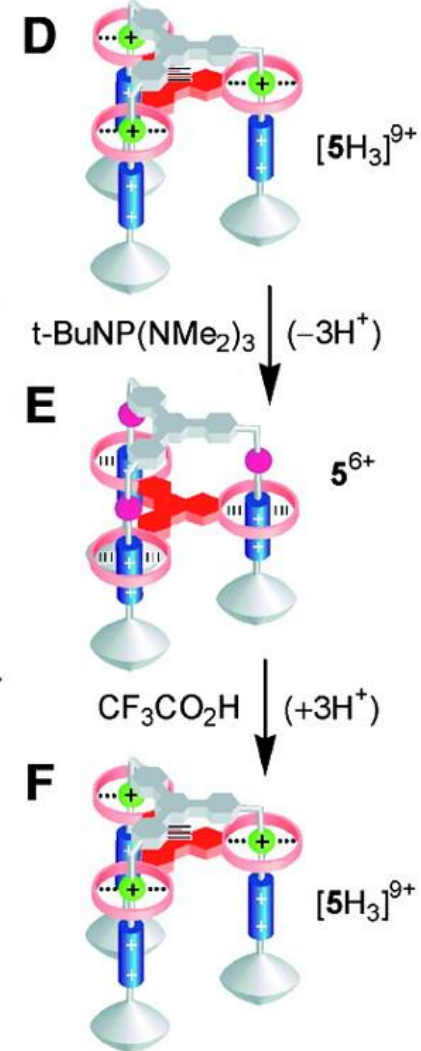
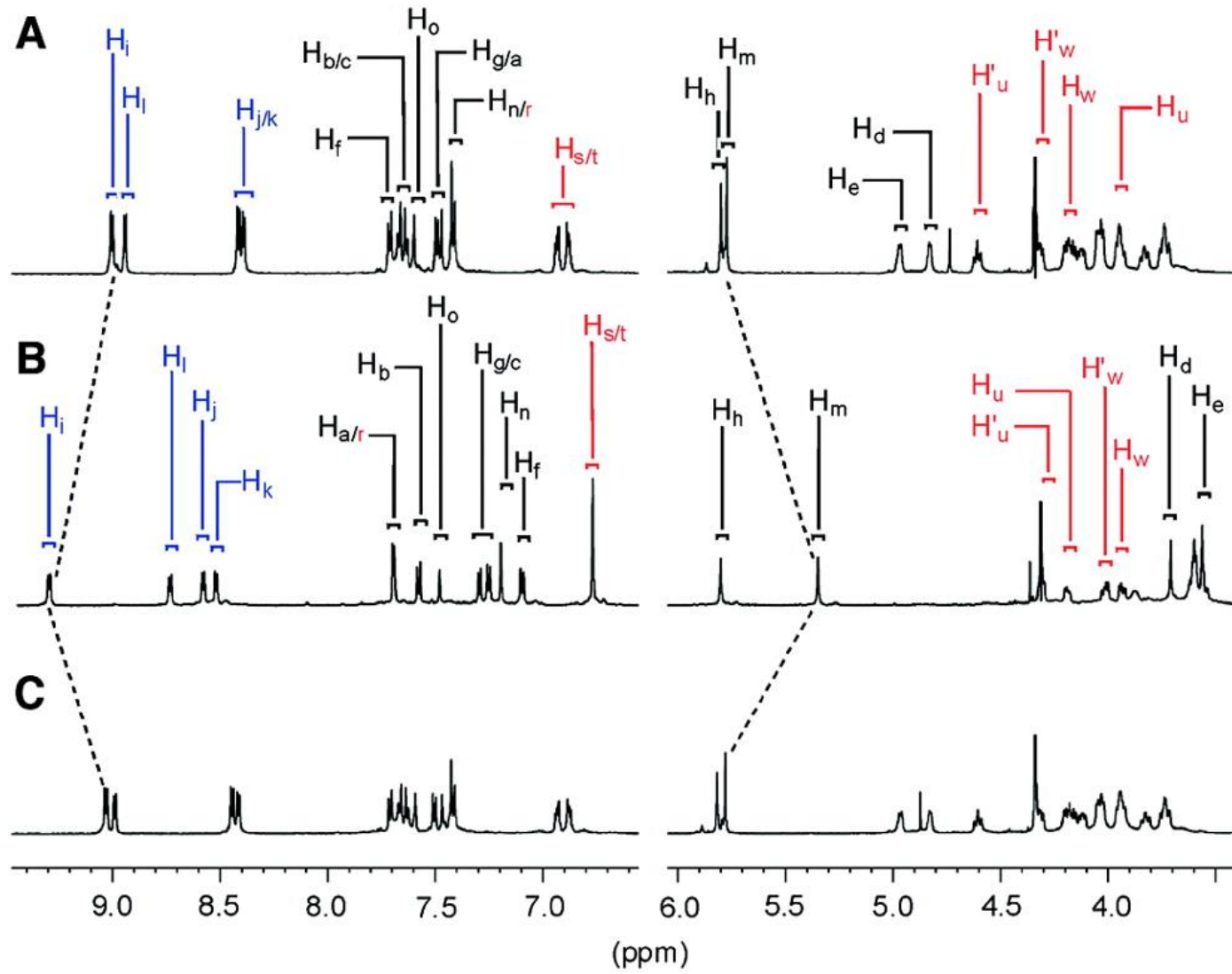


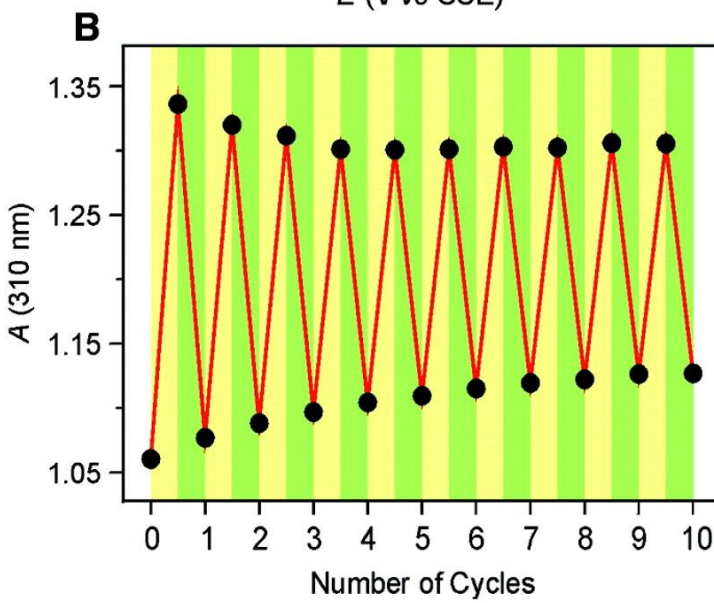
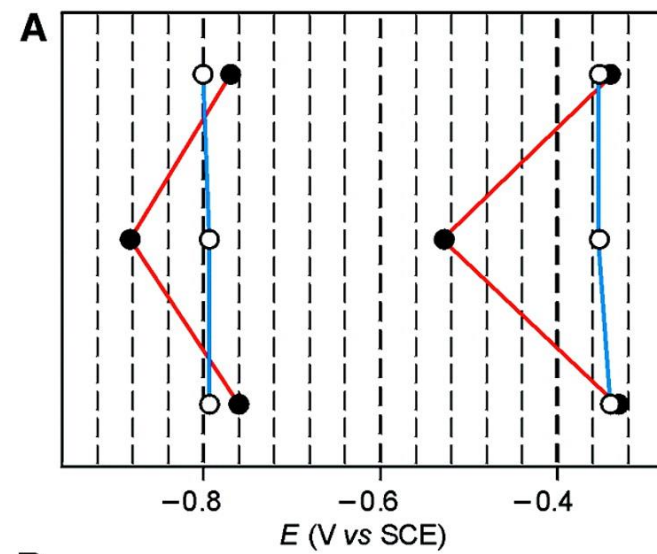
Weak $\text{C-H} \cdots \text{O}$

$\pi - \pi$









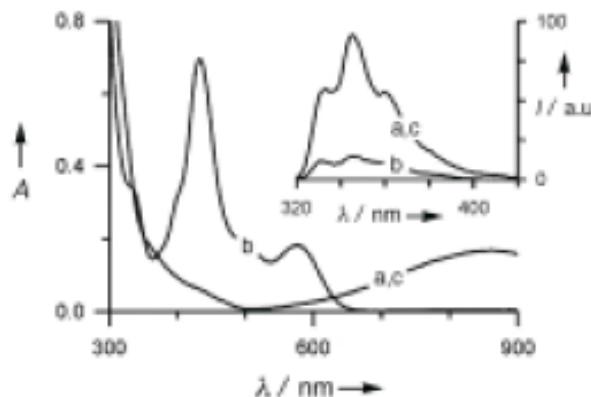
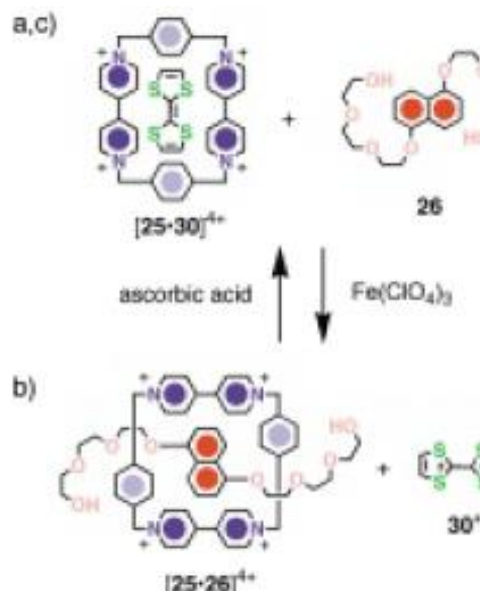
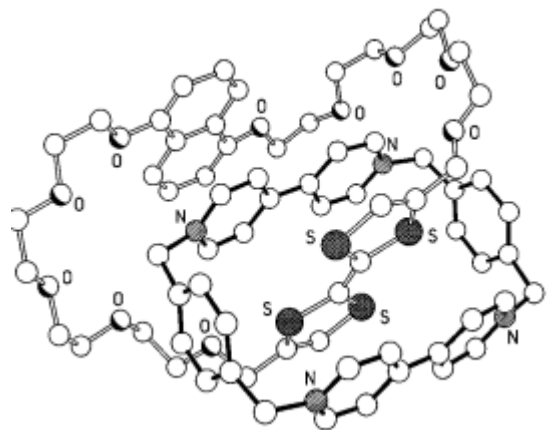
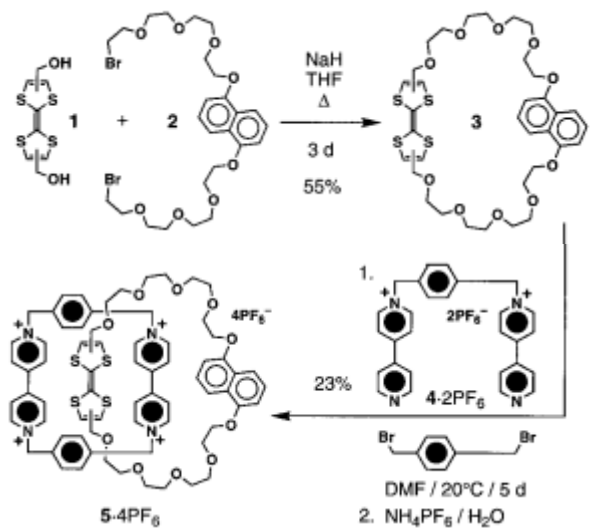
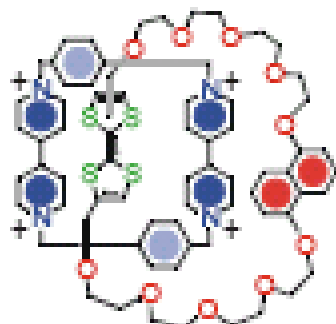


Figure 4. Top: the chemically induced interchange of guests **26** and **30** into the cavity of cyclophane **25**⁴⁺.^[93] Bottom: absorption and (inset) fluorescence ($\lambda_{\text{exc}} = 295 \text{ nm}$) spectra of a) a $5 \times 10^{-5} \text{ M}$ aqueous solution (298 K) of **[25-30]⁴⁺** and **26**; b) the same solution after addition of one equivalent of $\text{Fe}(\text{ClO}_4)_3$; c) solution b) after addition of one equivalent of ascorbic acid.

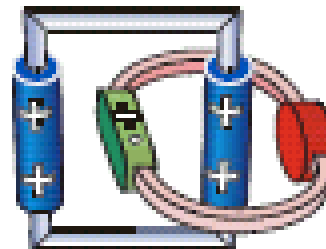


Input elettrochimico

Tetratiofulvalene (0)



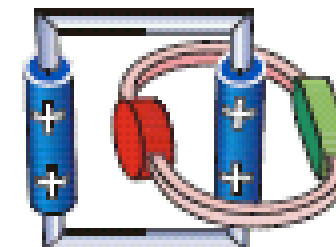
Tetratiofulvalene (+)



ossidazione

$+e^-$

riduzione



Tetratiofulvalene (0)

Tetratiofulvalene (+)

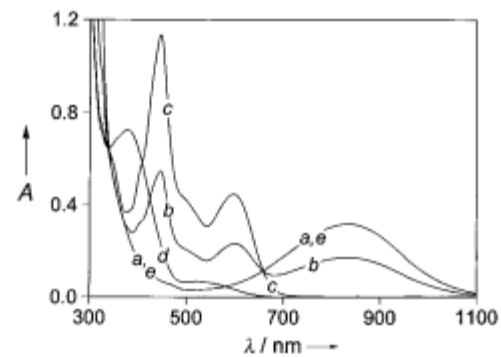
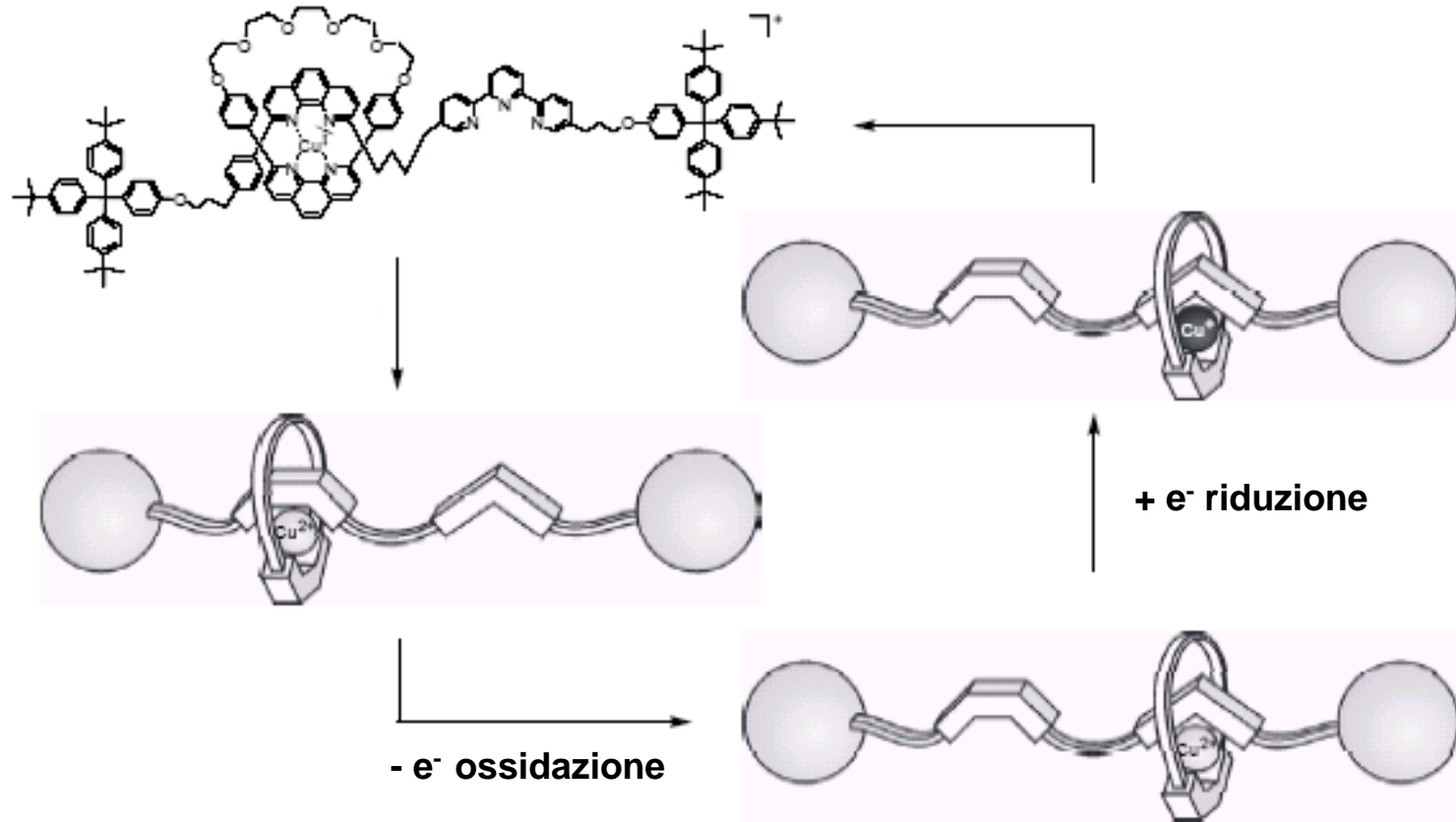
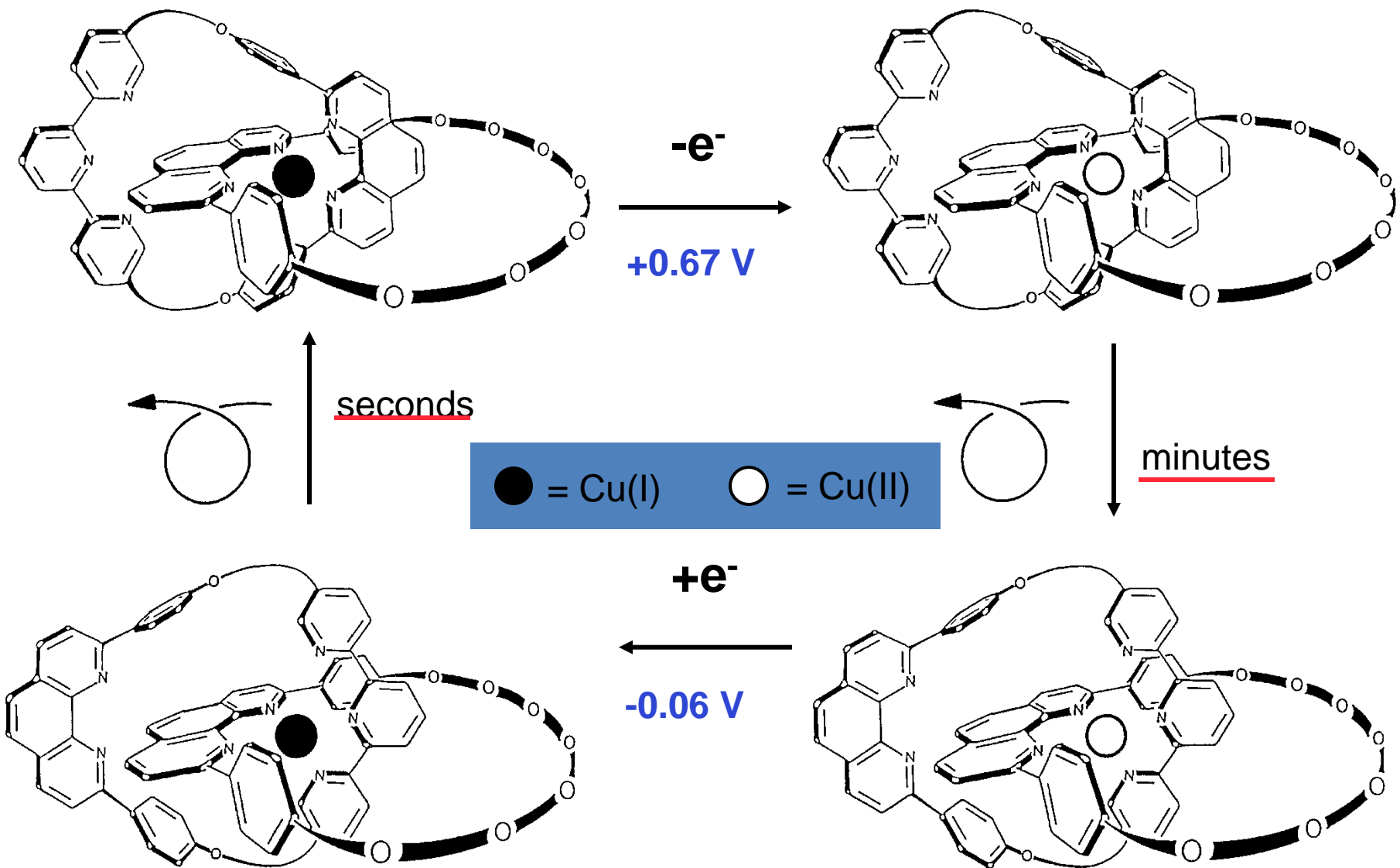


Figure 2. Absorption spectra (MeCN, 298 K) of a 9×10^{-5} M solution of [2]catenane **5**⁴⁺ (curve a) and of the same solution after addition of 0.4, 1.0, and 2.0 equiv of $\text{Fe}(\text{ClO}_4)_3$ (curves b–d). Addition of 2 equiv of ascorbic acid gives back the original spectrum (curve c).

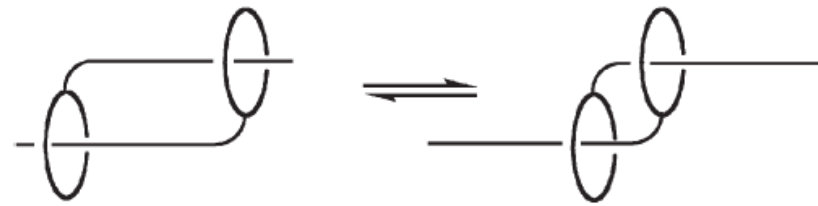
Input elettrochimico

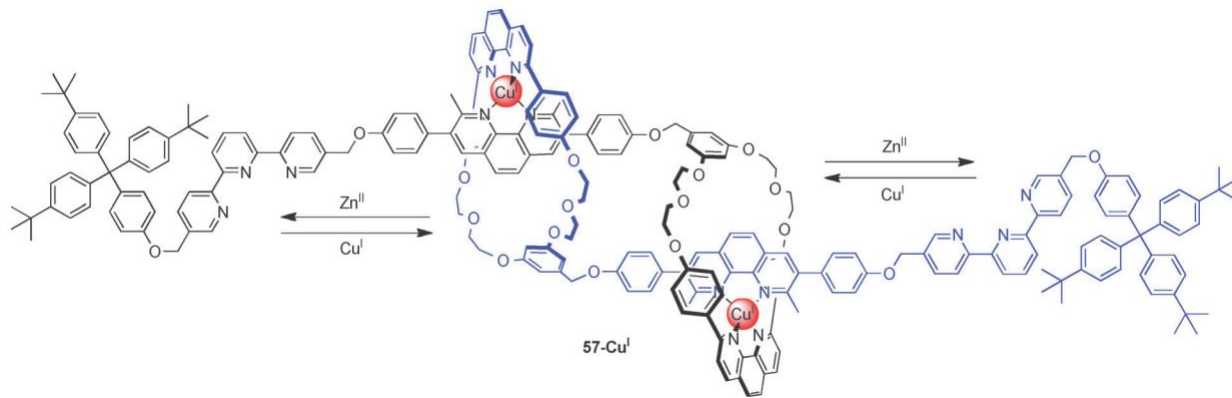
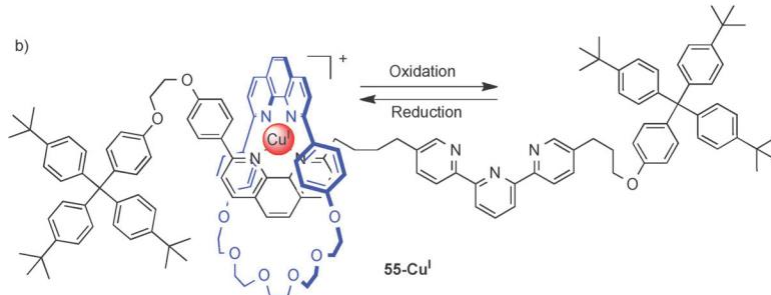
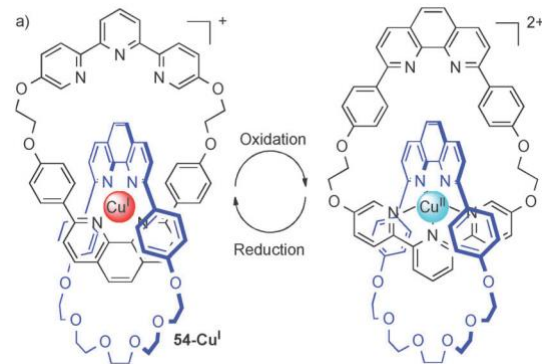


Input elettrochimico



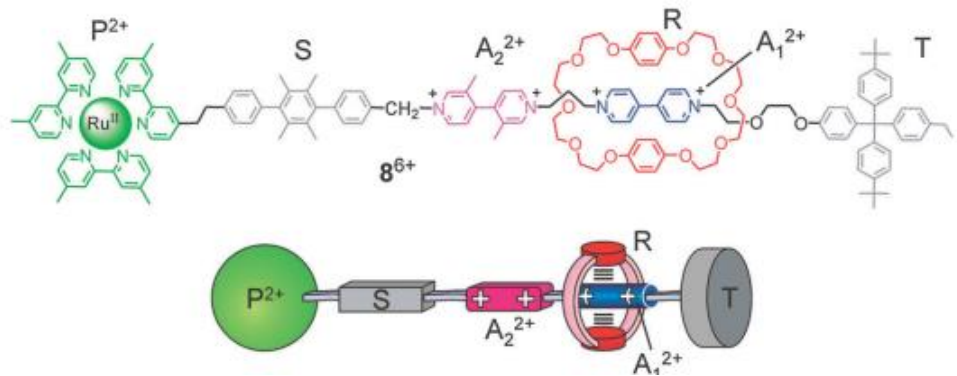
Input chimico



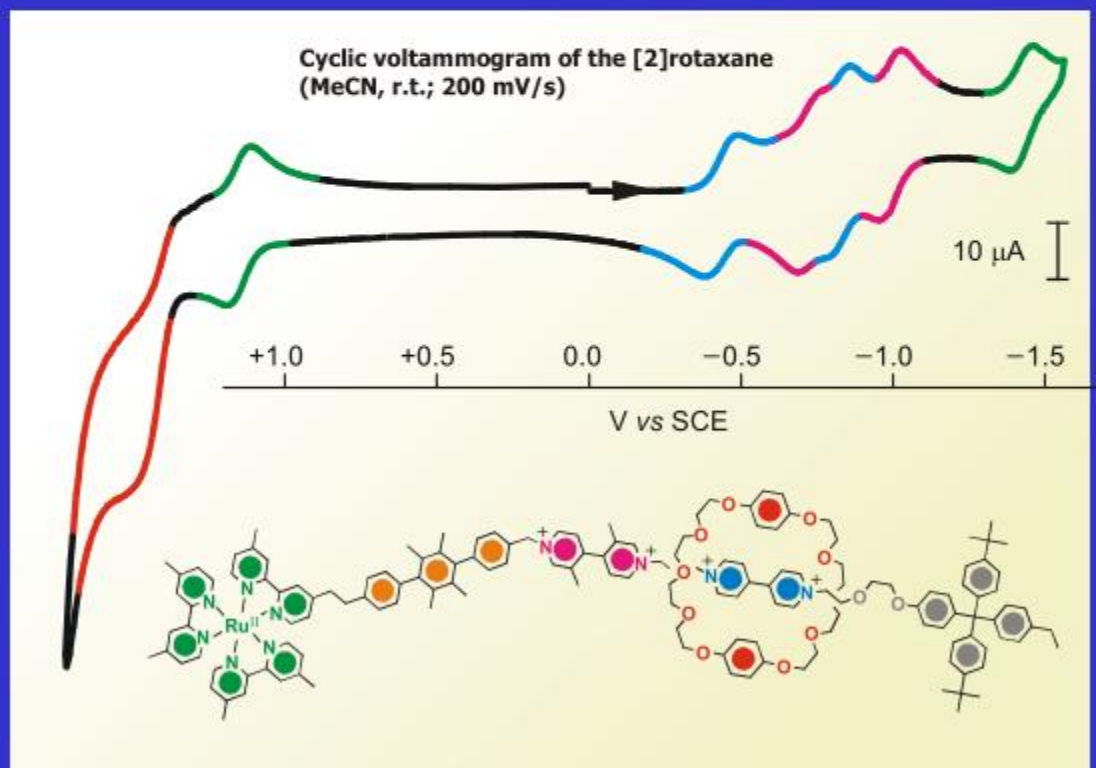
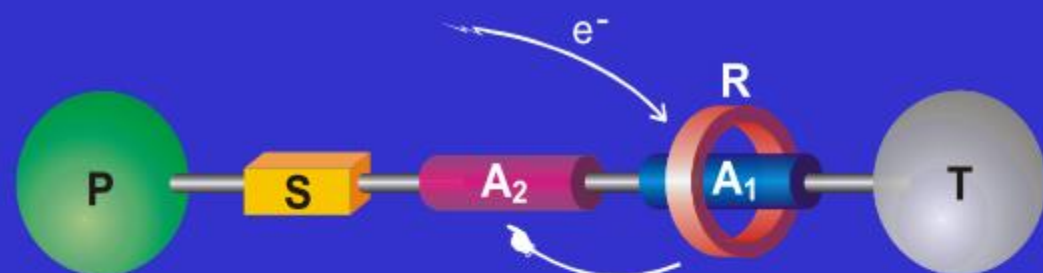


Input fotochimico

Ru(II)polypyridine complex (P^{2+})
p-terphenyl-type rigid spacer (S)
4,4'-bipyridinium (A_1^{2+})
3,3'-dimethyl-4,4'-bipyridinium (A_2^{2+})
Tetraarylmethane group (T)
Six PF_6^- counterions

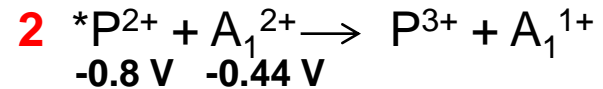
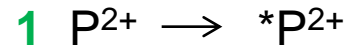
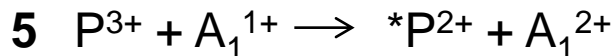
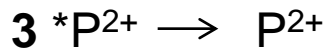
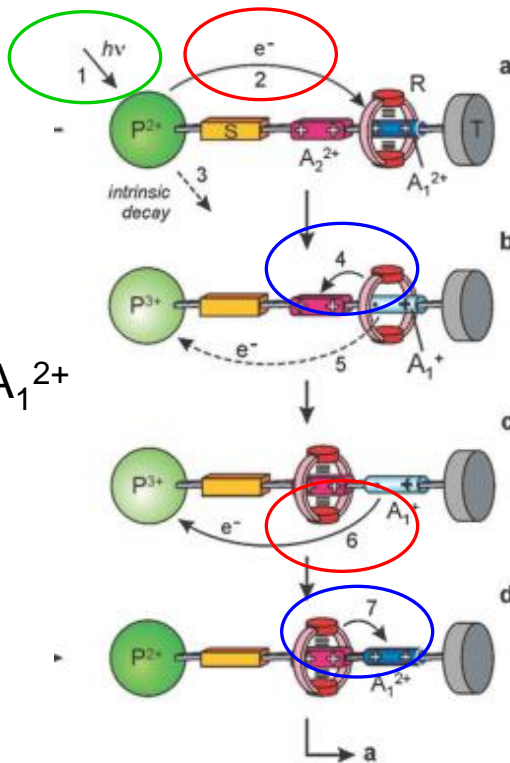
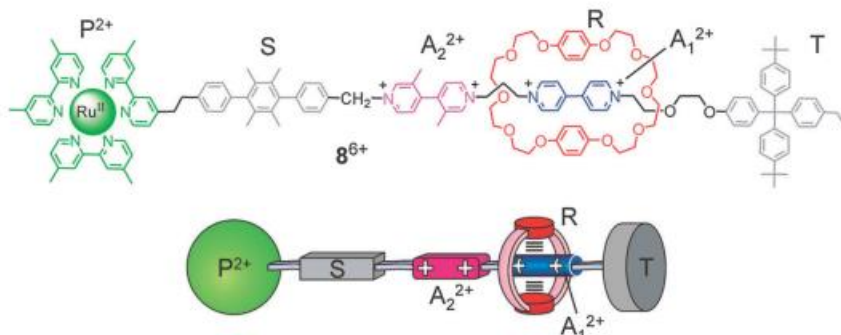


a) Redox-induced ring motion

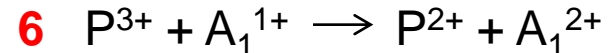


Input fotochimico

Ru(II)polypyridine complex (P^{2+})
 p -terphenyl-type rigid spacer (S)
 4,4'-bipyridinium (A_1^{2+})
 3,3'-dimethyl-4,4'-bipyridinium (A_2^{2+})
 Tetraarylmethane group (T)
 Six PF_6^- counterions

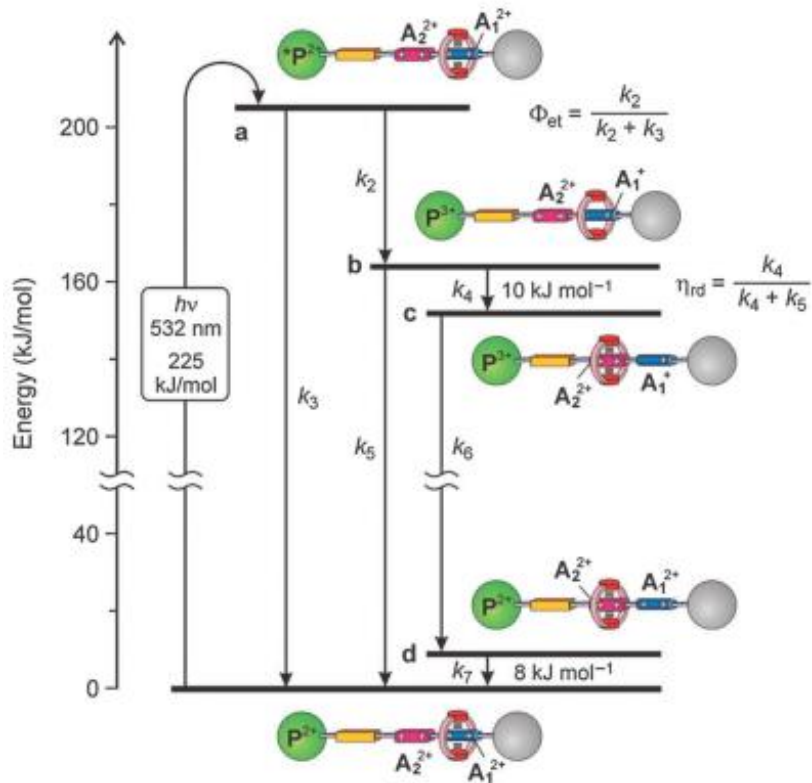


4 Shuttling (5 nm)



7 Shuttling (5 nm)

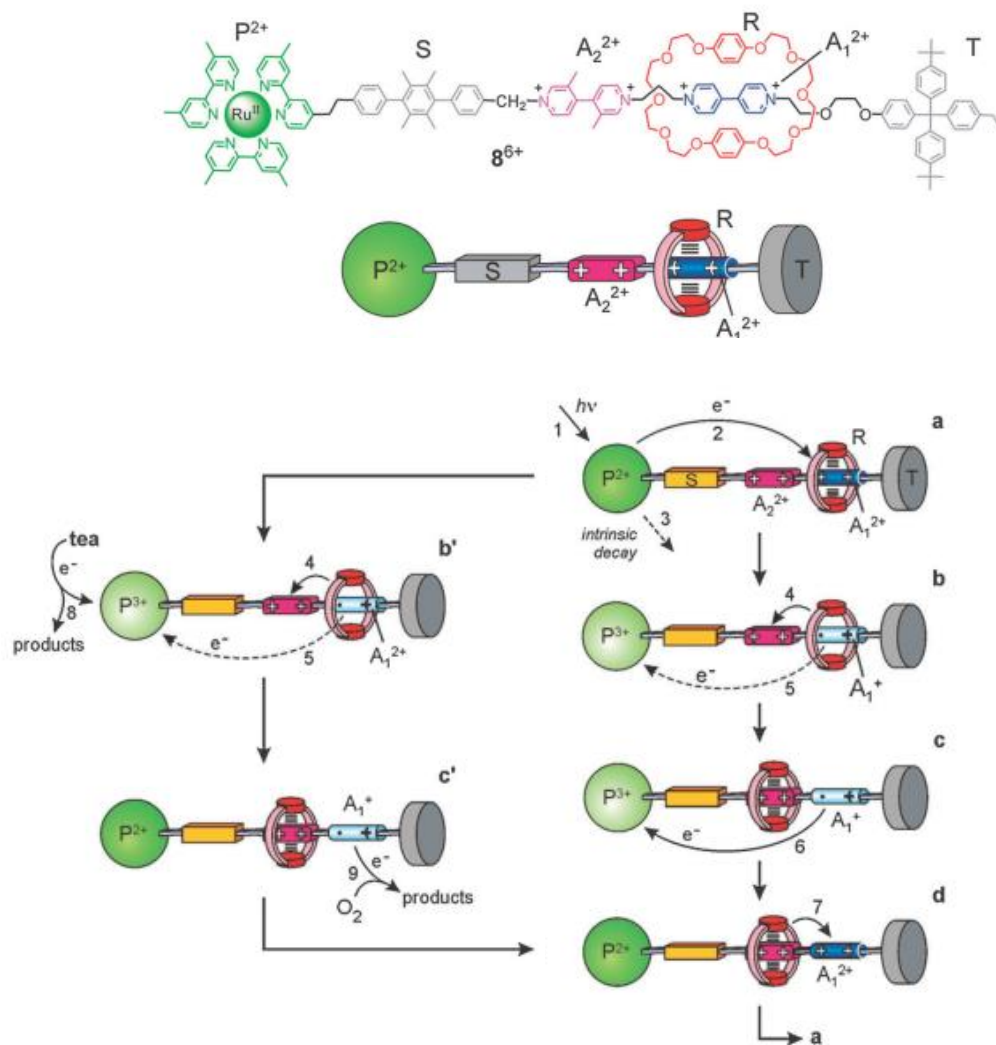
Input fotochimico



Hence, the fraction F of the excited state energy (205 kJ mol^{-1}) used for the motion of the ring amounts to *ca.* 10%, and the overall efficiency of the machine is $\eta = \Phi_{\text{sh}} \times F = 0.2\%$.

This somewhat disappointing result is compensated by the fact that the investigated system gathers together the following features: (i) it is powered by visible light (in other words, sunlight); (ii) it exhibits autonomous behaviour (*i.e.*, like natural molecular motors, it operates automatically in a constant environment as long as the energy source is available); (iii) it does not generate waste products; (iv) its operation can rely only on intramolecular processes, allowing in principle operation at the single-molecule level; (v) it can be driven at a frequency of about 1 kHz; (vi) it works in mild environmental conditions (*i.e.*, fluid solution at ambient temperature); and (vii) it is stable for at least 10^3 cycles.

Input fotochimico e chimico (agenti sacrificali TEA e O₂)



Input fotochimico

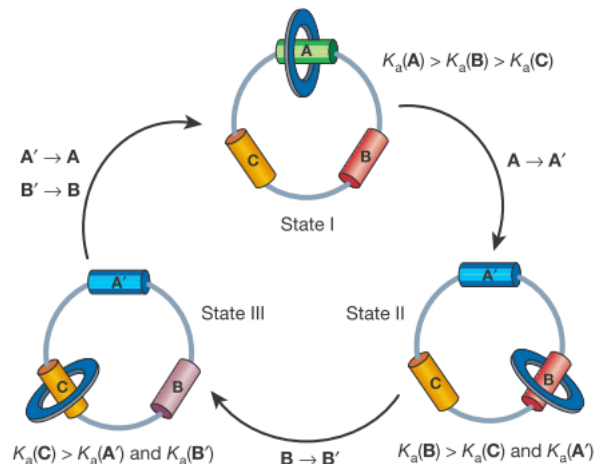
.....

Unidirectional rotation in a mechanically interlocked molecular rotor

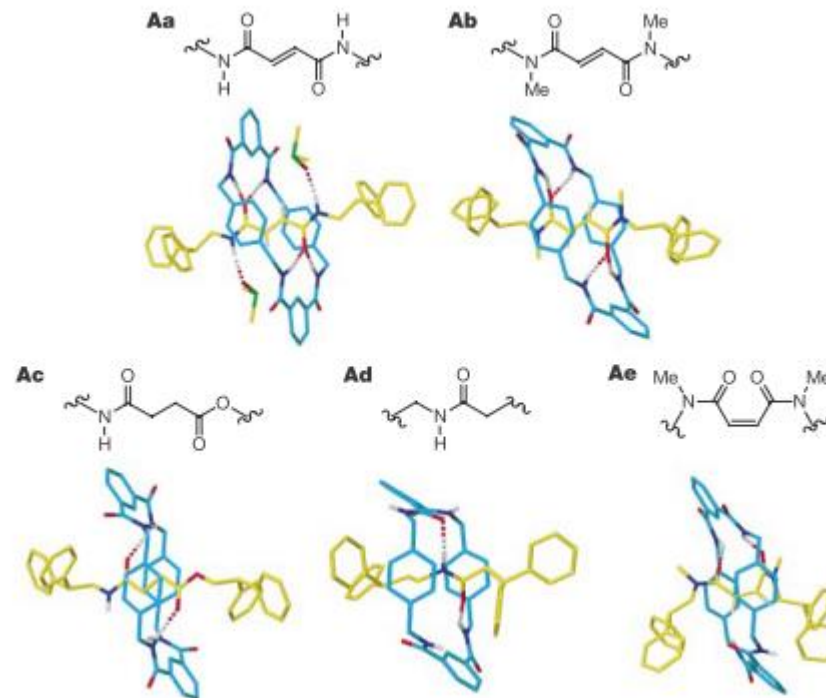
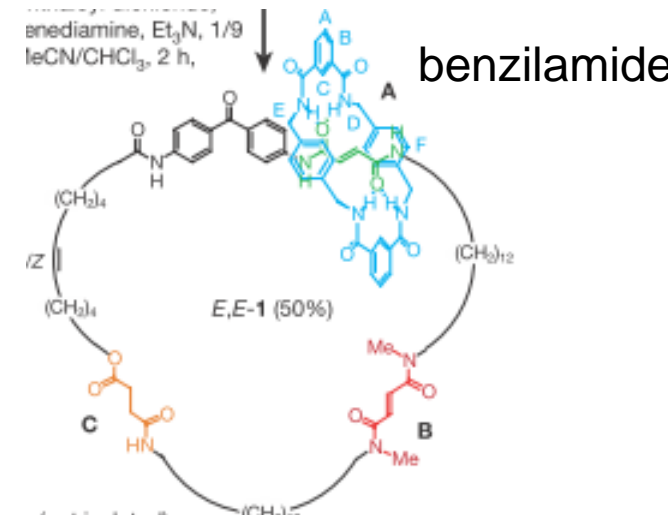
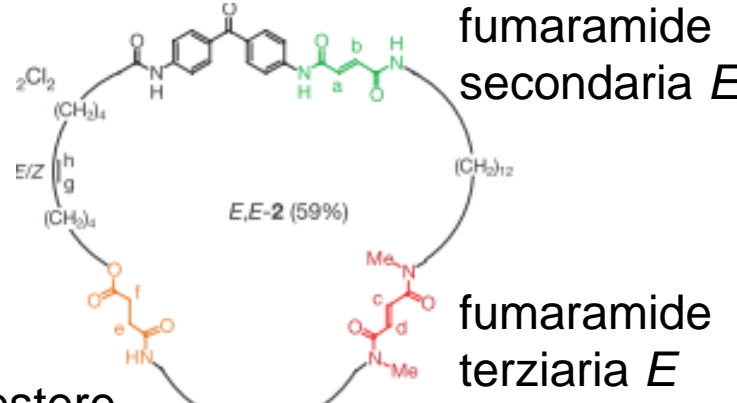
David A. Leigh*, Jenny K. Y. Wong*, François Dehez†
& Francesco Zerbetto†

* School of Chemistry, University of Edinburgh, The King's Buildings, West Mains Road, Edinburgh EH9 3JJ, UK

† Dipartimento di Chimica 'G. Ciamician', Università degli Studi di Bologna,
via F. Selmi 2, 40126 Bologna, Italy



benzofenone



Strutture ai raggi X dei siti di binding
dei modelli [2] rotaxani con indicati
i legami idrogeno (in ordine di affinità)

